Structural organization of essential iron-sulfur clusters in the evolutionarily highly conserved ATP-binding cassette protein ABCE1

Barthelme, Dominik; Scheele, Urte; Dinkelaker, Stephanie; Janoschka, Adam; MacMillan, Fraser; Albers, Sonja-Verena; Driessen, Arnold J. M.; Stagni, Marco Salamone; Bill, Eckhard; Meyer-Klaucke, Wolfram

Published in:
The Journal of Biological Chemistry

DOI:
10.1074/jbc.M700825200

Publication date:
2007

THE JOURNAL OF BIOLOGICAL CHEMISTRY VOL. 282, NO. 19, pp. 14598–14607, May 11, 2007

Structural Organization of Essential Iron-Sulfur Clusters in the Evolutionarily Highly Conserved ATP-binding Cassette Protein ABCE1*

Received for publication, January 29, 2007, and in revised form, March 12, 2007 Published, JBC Papers in Press, March 12, 2007, DOI 10.1074/jbc.M700825200

Dominik Barthelme[‡], Urte Scheele[‡], Stephanie Dinkelaker[‡], Adam Janoschka[§], Fraser MacMillan[¶], Sonja-Verena Albers[‖], Arnold J. M. Driessen[‖], Marco Salamone Stagni[**], Eckhard Bill[‡‡], Wolfram Meyer-Klaucke[**], Volker Schünemann[§], and Robert Tampé[‡1]

From the [‡]Institute of Biochemistry, Biocenter, Johann Wolfgang Goethe University, Max-von-Laue-Strasse 9, D-60439 Frankfurt am Main, Germany, the [§]Department of Physics, University of Kaiserlautern, Erwin-Schrödinger-Strasse 56, D-67663 Kaiserslautern, Germany, [¶]Institute of Physical and Theoretical Chemistry, Johann Wolfgang Goethe University, Max-von-Laue-Strasse 9, D-60439 Frankfurt am Main, Germany, the [‖]Department of Molecular Microbiology, University of Groningen, Kerklaan 30, 9751 NN Haren, The Netherlands, [**]European Molecular Biology Laboratory, Outstation Hamburg at DESY, Notkestrasse 85, D-22603 Hamburg, Germany, and [‡‡]Max Planck Institute for Bioinorganic Chemistry, Stiftstrasse 34-36, D-45470 Mülheim an der Ruhr, Germany

The ABC protein ABCE1, formerly named RNase L inhibitor RLI1, is one of the most conserved proteins in evolution and is expressed in all organisms except eubacteria. Because of its fundamental role in translation initiation and/or ribosome biosynthesis, ABCE1 is essential for life. Its molecular mechanism has, however, not been elucidated. In addition to two ABC ATPase domains, ABCE1 contains a unique N-terminal region with eight conserved cysteines, predicted to coordinate iron-sulfur clusters. Here we present detailed information on the type and on the structural organization of the Fe-S clusters in ABCE1. Based on biophysical, biochemical, and yeast genetic analyses, ABCE1 harbors two essential diamagnetic $[4Fe\text{-}4S]^{2+}$ clusters with different electronic environments, one ferredoxin-like ($CPX_nCX_2CX_2C$; Cys at positions 4–7) and one unique ABCE1-type cluster ($CXPX_2CX_3CX_nCP$; Cys at positions 1, 2, 3, and 8). Strikingly, only seven of the eight conserved cysteines coordinating the Fe-S clusters are essential for cell viability. Mutagenesis of the cysteine at position 6 yielded a functional ABCE1 with the ferredoxin-like Fe-S cluster in a paramagnetic $[3Fe\text{-}4S]^{+}$ state. Notably, a lethal mutation of the cysteine at position 4 can be rescued by ligand swapping with an adjacent, extra cysteine conserved among all eukaryotes.

Iron-sulfur (Fe-S)[2] clusters constitute an ancient prosthetic group, which can be found in proteins from all living organisms. They are only composed of the inorganic components sulfur and iron. In the most common cluster variants, [2Fe-2S], [3Fe-4S], and [4Fe-4S], the metal ions are directly coordinated by the inorganic sulfur and the adjunct cysteinyl groups from the protein backbone (1). Nevertheless, amino acids like histidine can also contribute to the iron coordination, as known for [2Fe-2S] Rieske clusters. Additionally, much more complicated structural arrangements can be found. The complex FeMoco and P-cluster of nitrogenase are just one example of clusters with higher nuclearity, arising from smaller substructures and clusters containing additional metal atoms like molybdenum (2). Furthermore, interconversion of Fe-S cluster is a widely distributed phenomenon, reflecting the dynamic arrangement and behavior (3). Despite their relative simple composition of only iron and sulfur (in most cases), Fe-S clusters are often essential components for the enzymatic function and are thereby involved in a vast variety of cellular processes. Beside their obvious role in electron transport, they operate as sensors for iron, for example, modulate protein stability, and play a role in nucleic acid binding and modification (1, 4).

Although Fe-S clusters can be synthesized *in vitro* (5), their assembly and maturation *in vivo* requires a highly complex and regulated machinery (6). Mitochondria are the central compartment in Fe-S cluster biogenesis, which is also the only essential function of this organelle known to date (6, 7). The underlying concept is not understood so far, because mitochondrial Fe-S cluster proteins are not essential for cell viability. The cytosolic, essential Fe-S protein ABCE1 could explain this phenomenon, because of the fact that Fe-S clusters can be transported from mitochondria to the cytosol (8, 9), where they are incorporated into the protein moiety.

ABCE1 is found evolutionarily conserved in all Archaea and Eukaryota, where it is essential for life (9–13). ABCE1 belongs to the superfamily of ATP-binding cassette (ABC) proteins with twin ABC ATPase domains, which are arranged in a head-to-tail orientation via a flexible linker and hinge region (14). Most of these members constitute membrane proteins that mediate ATP-driven unidirectional transport of a variety of molecules across biological membranes. Because ABCE1 does not contain any transmembrane domain, its function cannot be related to a membrane transport process. The protein was orig-

* The costs of publication of this article were defrayed in part by the payment of page charges. This article must therefore be hereby marked "*advertisement*" in accordance with 18 U.S.C. Section 1734 solely to indicate this fact.
[1] To whom correspondence should be addressed. Tel.: 49-69-798-29475; Fax: 49-69-798-29495; E-mail: tampe@em.uni-frankfurt.de.
[2] The abbreviations used are: Fe-S, iron-sulfur; ABC, ATP-binding cassette; ESEEM, electron spin echo envelope modulation; EXAFS, extended x-ray absorption fine structure; TXRF, total X-ray reflection fluorescence; WT, wild type; XAS, x-ray absorption spectroscopy; FT, Fourier transformation; T, tesla.

inally identified as the RNase L inhibitor in the innate immune response and therefore called RLI1 (15). It was subsequently shown that the assembly of the human immunodeficiency virus type 1 capsids requires ABCE1 in a strictly ATP-dependent manner (16). Very recently, an even more fundamental and general role was proposed in the process of translation initiation and ribosome biosynthesis (9, 12, 13, 17). ABCE1 was found to interact with translation initiation factors, eIF2, eIF3, eIF5, the 40 S ribosomal subunit, and several ribosomal RNAs. Depletion of the protein causes defects in the assembly of the preinitiation complex, rRNA processing, and accumulation of ribosomal subunits in the nucleus. Nevertheless, the underlying molecular mechanism remains enigmatic.

ABCE1 harbors a unique N-terminal region, including eight conserved cysteine residues with the $CX_4CX_3CX_3CPX_nCX_2$-CX_2CX_3P consensus sequence. A specific incorporation of iron, the interaction with members of the Fe-S cluster assembly machinery, and the functional importance of two of these eight cysteine residues (at positions 3 and 7) have been demonstrated (9). However, information regarding the type and structural organization of the Fe-S cluster has not been available until now.

By using homologously and heterologously expressed ABCE1 from the hyperthermophilic crenarchaeote *Sulfolobus solfataricus*, we provide detailed information on the Fe-S clusters. Highlighted by functional studies in yeast, we show the pivotal role of conserved cysteines coordinating the prosthetic group. We finally present a model for the structural organization of the Fe-S clusters in this essential and evolutionarily conserved protein.

EXPERIMENTAL PROCEDURES

Expression of ABCE1 in S. solfataricus—For overexpression of affinity-tagged ABCE1, a stable and selectable shuttle vector based on the virus SSV1 of *Sulfolobus shibatae* was used (18). The open reading frame SSO0287 (*abce1*) was amplified by PCR using genomic DNA of *S. solfataricus* and the primers, P1f 5′-CCATATCCCATGGTGAGAGTTGC-3′ and P4r 5′-GGG-CCCTTAATGGTGATGGTGATGGTGATGGTGTTTTTC-AAATTGTGGATGTACCAATTCTGGGTAGAAAGAA-3′. This resulted in the introduction of NcoI and ApaI restriction sites in the flanking regions of the gene and a tandem affinity (His_8 and StrepII) tag at the C terminus. The gene was cloned into pSVA5 (18), using the NcoI and ApaI sites yielding pSVA30. To transfer the *ara*S promoter together with the gene to be expressed into the virus-based vector, the BlnI/EagI insert from pSVA30 was ligated into pMJ02 (19), resulting in the plasmid pSVA31. Electroporation of *S. solfataricus pyr*EF mutant PH1–16 with pSVA31 and the isolation of single transformants were carried out as described (20, 21). Integration of the viral vector into the genome was confirmed by Southern blot analysis using standard procedures. *S. solfataricus* PH1–16 cells (21) harboring pSVA31 were inoculated in 50 ml of Brock's medium containing 0.1% tryptone. After 2 days of growth ($A_{600} \sim 0.5$) at 80 °C and pH 3.5, these cells (10 ml) were transferred to 400 ml of medium containing 0.1% tryptone and 0.2% arabinose to induce expression of ABCE1. After 2 days of growth ($A_{600} \sim 0.8$), the cells were harvested and resuspended in 10 mM Tris-HCl, 100 mM NaCl, pH 7.4.

Expression of S. solfataricus ABCE1 in Escherichia coli—The open reading frame SSO0287 of *S. solfataricus* ABCE1 was amplified by PCR using genomic DNA of S. solfataricus and the primers, P1f 5′-CCATATCCCATGGTGAGAGTTGC-3′ and P1r 5′-CCATATGGATCCCTGGGTAGAAAGAACCAAG-GAG-3′, and cloned into the NcoI and BamHI sites of the pSA4 expression vector (22). The resulting plasmid (pSD1) codes for wild type ABCE1 of *S. solfataricus* with a C-terminal His_6 tag. The two conserved cysteines, Cys-24 and Cys-54, were individually exchanged for serine residues (C24S and C54S) by QuikChange site-directed mutagenesis (Stratagene). PCR and mutagenesis products were confirmed by DNA sequencing. The *E. coli* strain BL21(DE3) (Novagen) was co-transformed with either of the ABCE1 constructs and the pRARE plasmid (Novagen) coding for rare tRNAs and grown in LB medium supplemented with 100 μg/ml ampicillin and 25 μg/ml chloramphenicol at 37 °C. Expression was induced at an A_{600} of 0.6 for 3 h at 30 °C by adding 0.2 mM isopropyl β-D-thiogalactopyranoside.

Purification of ABCE1—All purification steps and experimental analysis were carried out under argon atmosphere or in an anaerobic chamber containing 95% N_2, 5% H_2 (Coy Laboratories). Before use, buffers were degassed and equilibrated inside the anaerobic chamber for several days. Cell pellets of *S. solfataricus* were resuspended in lysis buffer A (20 mM NaH_2PO_4, 300 mM NaCl, 20 mM imidazole, pH 7.4), disrupted by using a Branson Sonifier 250 at 60% output in eight pulses of 30 s on ice, and centrifuged for 30 min at 114,000 × *g*. Afterward, ABCE1 was purified to homogeneity via metal affinity chromatography (HisSelect, Sigma) by washing/elution with 20 mM, 300 mM imidazole. For purification of ABCE1 expressed in *E. coli*, frozen cells were thawed, resuspended in lysis buffer B (20 mM Tris-HCl, 100 mM NaCl, 1 mM dithiothreitol, 1 mM EDTA, pH 7.4), and disrupted by sonication as described before. After centrifugation at 114,000 × *g* for 30 min, the supernatant was heated at 70 °C for 10 min and additionally centrifuged for 1 h at 114,000 × *g*. The solution was subsequently applied to metal affinity chromatography (HisTrap, GE Healthcare). ABCE1 was purified by washing/elution with 60 mM, 200 mM imidazole. Protein fractions were exchanged to buffer C (20 mM Tris-HCl, 100 mM NaCl, pH 7.4) using a Centricon device (Millipore). The protein concentration was determined by the Coomassie Plus™ Bradford assay (Pierce) using bovine serum albumin as a standard.

Determination of Iron and Sulfur—Total reflection x-ray fluorescence (TXRF) as a trace multielement analytical method was applied to quantify the iron and sulfur content of purified ABCE1. The measurement was carried out using an EXTRA IIA spectrometer (Atomica Instruments) with a sample volume of 4 μl in 50 mM Tris acetate buffer, pH 7.5. 20 μl of protein solution were placed onto siliconized quartz carrier plates and evaporated to dryness. By excitation with the Mo(K_α) line for 1000 s, a multielement fluorescence spectrum was obtained. The intensities of the sulfur and iron peaks were related to a rubidium peak as an internal standard. The iron content of ABCE1 was further determined colorimetrically by the method of

Fish (23), and the inorganic sulfur was quantified according to Beinert (24).

UV-visible Spectroscopy—Spectra of wild type and ABCE1 mutants were recorded on a Cary 50 spectrophotometer (Varian) in buffer C. ABCE1 was titrated with sodium dithionite or freshly prepared potassium ferricyanide (both in buffer C). The spectra of the oxidant and reductant solutions alone were subtracted from the corresponding curves.

EPR Spectroscopy—ABCE1 was analyzed by continuous wave EPR, either untreated, reduced with sodium dithionite or ascorbate, or oxidized with potassium ferricyanide in buffer C. X-band EPR spectra were measured on a Bruker E-500 eleXsys spectrometer using a standard rectangular Bruker EPR cavity equipped with an ESR900 helium flow cryostat (Oxford Instruments). The spectra were recorded under the following experimental conditions: microwave frequency, 9.424 GHz; microwave power, 8 milliwatts; field modulation frequency, 100 kHz; field modulation depth, 5 G (peak to peak); temperature, 10 K.

To study the immediate environment around the Fe-S cluster, pulsed EPR was performed on a Bruker E-580 spectrometer using a Bruker EPR cavity (MD5-W1) equipped with a helium flow cryostat (CF935, Oxford Instruments). The pulses were amplified using a 1-kilowatt pulsed traveling wave tube amplifier. A conventional two-pulse ($\pi/2$-τ-π) sequence was used. A two-pulse, echo modulation experiment (ESEEM) was performed by integrating the area under the Hahn echo as a function of time between the two microwave pulses. The frequency domain spectrum was obtained by Fourier transformation of the time domain trace after subtraction of a mono-exponential decay function. This measurement was performed at 10 K at a microwave frequency of 9.745 GHz using a $\pi/2$ pulse length of 8 ns, a starting τ of 132 ns, and a short repetition rate of 1 ms.

Mössbauer Spectroscopy—For preparation of the Mössbauer sample, metallic ^{57}Fe (96% enrichment; Chemotrade) was dissolved in 37% (v/v) HCl at 80 °C for several days. The obtained $^{57}FeCl_3$ solution was directly added to the *S. solfataricus* medium (without $FeCl_3$) to a final concentration of 41 μM. Mössbauer spectra of purified ABCE1 were recorded in buffer C by using a conventional spectrometer in the constant acceleration mode. Isomer shifts are given relative to α-Fe at room temperature. Zero-field spectra were measured in bath cryostat (Oxford Instruments), whereas for the high field spectra (4 T $\perp$ γ), a cryostat equipped with a superconducting magnet was used (Oxford Instruments). Magnetically split spectra were simulated within the spin Hamilton formalism (25); otherwise, spectra were analyzed by least square fits using Lorenzian line shape.

X-ray Absorption Spectroscopy (XAS)—ABCE1 was concentrated to 1.2 mM in iron. Afterward, XAS sample was filled into the 25-μl plastic XAS cuvettes and stored at cryogenic temperatures. The *K*-edge iron x-ray absorption spectrum was recorded at the beam line D2 of the EMBL Outstation Hamburg at DESY (Germany). The DORIS storage ring operated at 4.5 GeV with the positron beam current ranging from 145 to 80 mA. A ^{111}Si double-crystal monochromator scanned x-ray energies around the iron *K*-edge (6.9–8.1 keV). Harmonic rejection was achieved by a focusing mirror (cut-off energy at 20.5 keV) and a monochromator detuning to 50% of its peak intensity. The sample cells were mounted in a two-stage Displex cryostat and kept at about 20 K. The x-ray absorption spectra were recorded as iron K_α fluorescence spectra with a Canberra 13-element germanium solid-state detector. Data reduction, such as background removal, normalization, and extraction of the fine structure, was performed with KEMP (26) assuming a threshold energy $E_{0,Fe}$ = 7120 eV. Sample integrity during exposure to synchrotron radiation was checked by monitoring the position and shape of the absorption edge on sequential scans. No changes were detectable. The extracted iron *K*-edge (25–860 eV) EXAFS data were analyzed as reported previously (27).

Functional Analysis of ABCE1 Mutants in Yeast—To investigate various cysteines mutants of ABCE1, we used a yeast strain, in which the endogenous promoter was replaced by a tetracycline-regulated one (28). The cells were transformed with the multicopy plasmid pRS423 harboring the wild type or ABCE1 mutants. A plasmid coding for *abce1* from *Saccharomyces cerevisiae* was generated by PCR using the primers P2f 5′-ATGGTCGACGCCCTCGTATCTGCAACG-3′ and P2r 5′-ATACCCGGGAGTACGGATCACCGAAGAGG-3′ with chromosomal DNA as a template. The amplified construct was inserted into the SalI and SmaI restriction sites of the vector pRS423. ABCE1 was expressed under the control of the endogenous promoter. The highly conserved N-terminal cysteine residues Cys-16, Cys-21, Cys-25, Cys-29, Cys-55, Cys-58, Cys-61, and Cys-65 as well as the cysteine Cys-38 were exchanged to serines or to alanines by site-directed mutagenesis. Single, double, and triple mutations were created and transformed into yeast cells. Following doxycycline treatment, the chromosomal expression of ABCE1 was repressed and the ABCE1 mutants substituted for the endogenous protein in the cells. The pRS423 vector containing the wild type *ABCE1* gene and the empty vector served as control plasmids.

RESULTS

Expression and Isolation of ABCE1—To analyze the structural organization and function of Fe-S clusters in ABCE1, we used a double tracked approach. (i) Functional studies of each cysteine in Fe-S cluster assembly of ABCE1 were performed in yeast. (ii) For biophysical and biochemical analyses of the Fe-S cluster, we chose ABCE1 from the hyperthermophilic crenarchaeote *S. solfataricus*. Notably, this thermostable protein contains only the eight conserved cysteines putatively coordinating Fe-S clusters. The yeast and archaeal protein are highly homologous (43% identity and 66% similarity, see also alignment of the N-terminal domain in Fig. 7*B*).

Based on a newly developed inducible expression system in *S. solfataricus* (18), ABCE1 was overexpressed and purified to homogeneity in quantities sufficient for biophysical studies (Fig. 1*A*). 0.5 mg of protein (68 kDa) was obtained from 1 liter of culture. Because of the unexpected finding of viable ABCE1 cysteine mutants, we transferred the corresponding mutations into ABCE1 from *S. solfataricus* for further analysis. Genetic manipulations in Archaea are still time-consuming and by far not a routine method. Therefore, wild type and the ABCE1 mutants were heterologously expressed in *E. coli* and purified to homogeneity as described above. In this case, 1–2 mg of

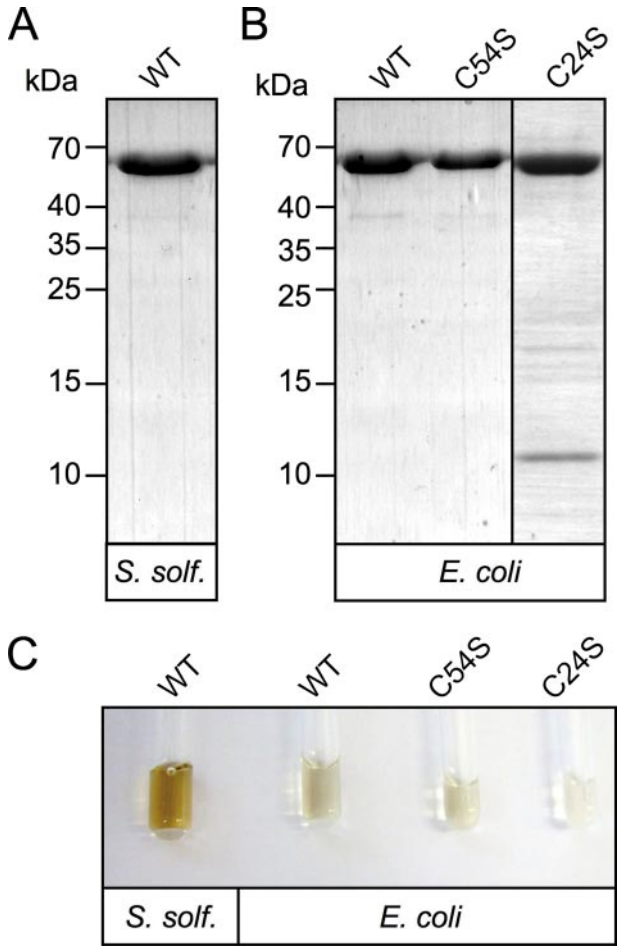

FIGURE 1. **Expression and purification of wild type and ABCE1 mutants.** WT ABCE1 expressed in *S. solfataricus* (*S. solf.*, *A*) and WT ABCE1, C54S, and C24S mutants heterologously expressed in *E. coli* (*B*) were purified under strictly anaerobic conditions via metal affinity chromatography and subsequently analyzed by SDS-PAGE (15%, Coomassie Blue). 0.5–1 mg of ABCE1 was isolated per liter of *S. solfataricus* culture, whereas the yield for the heterologous system was ~2 mg/liter. *C*, WT ABCE1 isolated from *S. solfataricus* (75 μM) or from *E. coli* (35 μM) as well as the C54S mutant (35 μM) showed a brownish color, except for the C24S mutant (35 μM).

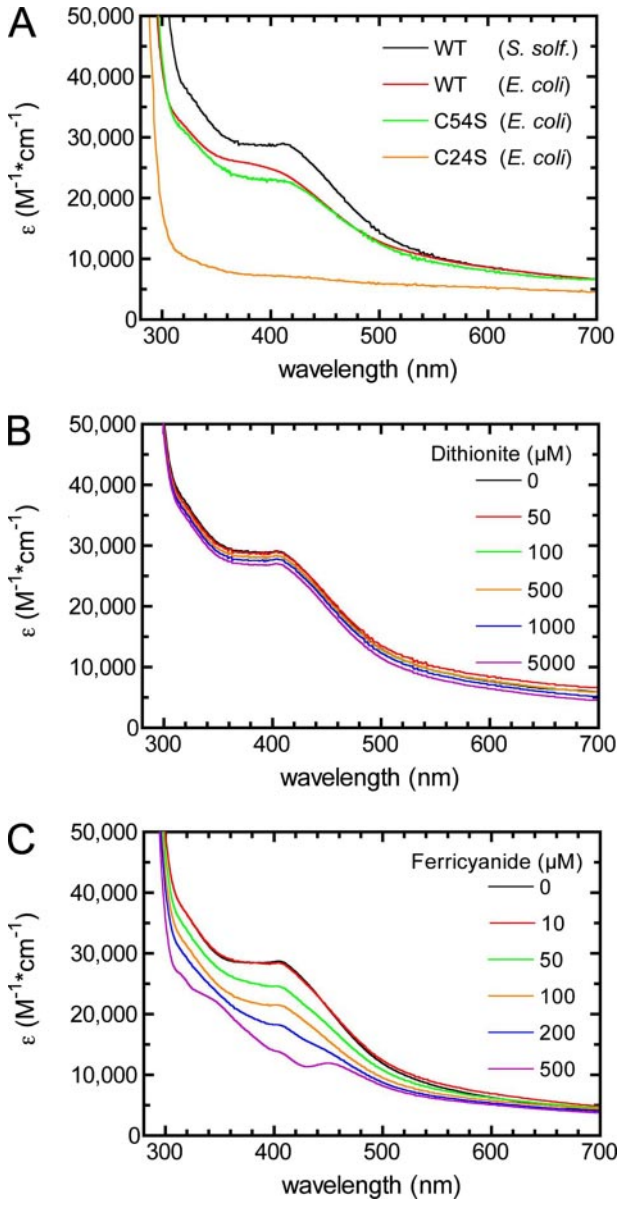

FIGURE 2. **UV-visible absorption spectroscopy of wild type and ABCE1 mutants.** *A*, spectra of WT ABCE1 isolated from *S. solfataricus* (*S. solf.*, *black line*) or from *E. coli* (*red line*) as well as the mutants C54S (*green line*) and C24S (*orange line*) were recorded in the buffer C. WT ABCE1 isolated from *S. solfataricus* was incubated with the reductant sodium dithionite (*B*) or the oxidant potassium ferricyanide (*C*) at the indicated concentrations for 2 min. All spectra were recorded at a protein concentrations of 50 μM.

protein was obtained from 1 liter of *E. coli* culture. Interestingly, some degradation products were copurified with the C24S mutant (Fig. 1*B*). This behavior is typical for Fe-S proteins, in which clusters are absent or not correctly assembled.

All ABCE1 preparations, except the C24S mutant, showed a brownish color, typical for Fe-S cluster proteins (Fig. 1*C*). After exposure to oxygen, the C54S mutant rapidly lost its color, whereas WT ABCE1 isolated either from *S. solfataricus* or *E. coli* remained brownish for at least several hours (data not shown).

Assembly of Two Fe-S Clusters in ABCE1—ABCE1 isolated from *S. solfataricus* exhibits a characteristic UV-visible spectrum with a maximum at 280 nm, a shoulder at 320 nm, and a broad peak around 410 nm (Fig. 2*A*), indicative for cubane [4Fe-4S]- or cuboidal [3Fe-4S]-type clusters (29). The molar extinction coefficient ϵ_{410} of 29,000 M^{-1} cm^{-1} is in the range of proteins containing two of these clusters (30). The absorption spectrum of WT ABCE1 isolated from *E. coli* differed only by the extinction coefficient ϵ_{410} of 24,000 M^{-1} cm^{-1} (17% reduction compared with ABCE1 isolated from *S. solfataricus*). Surprisingly, the C54S mutant showed an absorption spectrum very similar to WT ABCE1 purified from *E. coli* (ϵ_{410} = 22,500 M^{-1} cm^{-1}), demonstrating that the assembly of the Fe-S clusters is comparable in both proteins. In contrast, the C24S mutant showed no specific absorption at 410 nm revealing a defect in Fe-S cluster assembly. As addressed below, the functional consequences of these mutations have been examined in yeast.

Titration of WT ABCE1 with the reductant sodium dithionite (Fig. 2*B*) or ascorbate (not shown) did not significantly change the UV-visible spectra. This demonstrates the stability of the Fe-S cluster at low redox potential. In contrast, titration with the oxidant potassium ferricyanide resulted in loss of the

410-nm peak and the appearance of new absorption bands at 340 and 450 nm (Fig. 2*C*). Remarkably, the C54S mutant exhibited a greater sensitivity to oxidation by ferricyanide as compared with WT ABCE1, resulting in an immediate loss of the absorption at 410 nm (data not shown).

We next quantified the amount of incorporated iron and sulfur in the WT and ABCE1 mutants by TXRF spectroscopy and colorimetric assays. WT ABCE1 (1 nmol) isolated from *S. solfataricus* contains 7.0 nmol of iron and 6.1 nmol of acid-labile sulfur per nmol of protein (Table 1). In comparison, WT ABCE1 purified from *E. coli* harbors 13% less iron (6.1 nmol) and 10% less acid-labile sulfur (5.5 nmol). Considering a small amount of impurities and the intrinsic error in protein quantification, it seems likely that the iron and sulfur content are slightly underestimated. Especially for the protein isolated from *E. coli,* a small population of nonassembled Fe-S cluster can be found.

Together with the UV-visible data, these findings clearly demonstrate the presence of two cubane or one cubane and one cuboidal Fe-S clusters in the ABCE1. The C54S mutant showed also incorporation of iron and acid-labile sulfur but with decreased values compared with WT ABCE1. It is worth mentioning that the Fe-S clusters in the C54S mutant were extremely labile, resulting in a loss of iron and sulfur during buffer exchange (*e.g.* dialysis). In the C24S mutant, no significant iron and acid-labile sulfur were detected, consistent with the colorless protein solution (Fig. 1*C*) and the UV-visible spectra (Fig. 2*A*). Importantly, no other metal ions such as copper, nickel, zinc, or molybdenum were found in all ABCE1 proteins by TXRF analysis.

ABCE1 Harbors Diamagnetic Fe-S Clusters—We next examined the Fe-S clusters in ABCE1 by EPR spectroscopy. The two Fe-S clusters found in ABCE1 are EPR-silent and therefore in a diamagnetic state (Fig. 3*A*). It should be mentioned that ABCE1 isolated from *S. solfataricus* or *E. coli* showed identical spectroscopic behavior (data not shown). Interestingly, oxidation of the same sample with ferricyanide leads to an EPR signal (Fig. 3*A*), which, based on the relatively isotropic *g*-tenors, is characteristic for the formation of a [3Fe-4S]$^{+}$ cluster (31, 32). Further addition of the oxidation reagent did not increase the EPR signal, which finally disappeared (data not shown). In agreement with the UV-visible spectra, the two diamagnetic Fe-S clusters in ABCE1 could not be reduced either by ascorbate (not shown) or by the strong reductant dithionite at pH 9.0 (Fig. 3*B*).

Notably, even without oxidation, the C54S mutant showed an EPR signal (with regard to *g*-tensors and spin intensity) similar to oxidized WT ABCE1 (Fig. 3*C*). In contrast to WT ABCE1, oxidation of the C54S mutant leads to a decrease in the EPR signal even at low concentrations of ferricyanide (Fig. 3*C*). The slight difference in the overall line shape of the C54S mutant and the oxidized wild type protein may result from a different electronic environment and the influence of the mutant on the *g*-tensor and/or some of the small proton hyperfine interactions, which determine this line shape. Indeed, two-pulse ESEEM experiments of the C54S mutant did not reveal any other magnetic nuclei (*e.g.* ^{14}N) in the immediate environment of the cluster (data not shown). In conclusion, ABCE1 contains two diamagnetic [4Fe-4S]$^{2+}$ clusters, one being converted into a [3Fe-4S]$^{+}$ state upon oxidation or cysteine mutagenesis.

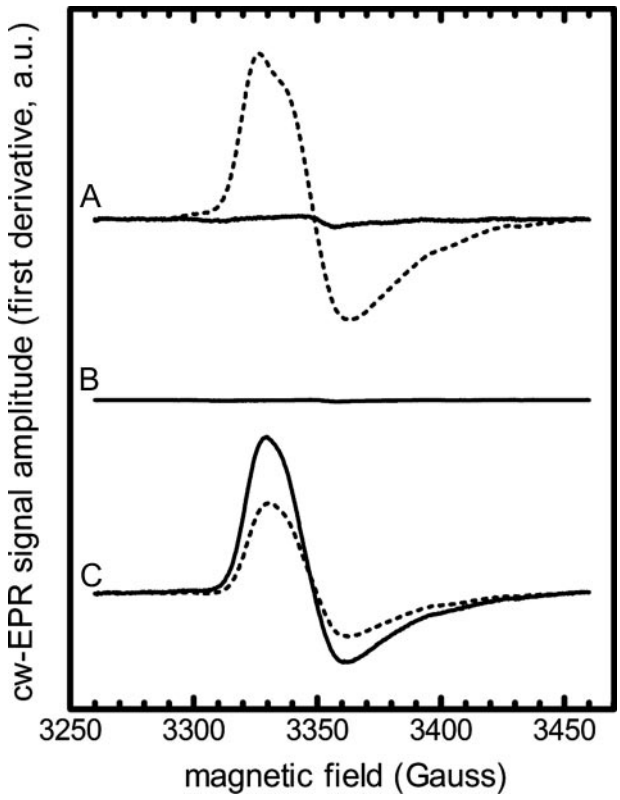

FIGURE 3. **EPR spectroscopy of wild type ABCE1 and C54S mutant.** *A,* EPR spectra of WT ABCE1 purified from *S. solfataricus* (*solid line*) were recorded in buffer C before (*solid line*) and after oxidation with a 10-fold excess of ferricyanide (*dotted line*). The *g*-tensor principal values of oxidized ABCE1 for *g*(1): 2.031, *g*(2): 2.017, *g*(3): 2.002 (error ± 0.002), extracted by numerical simulation (data not shown), are indicative for a [3Fe-4S]$^{+}$ cluster. *B,* spectra of WT ABCE1 reduced with 50-fold molar excess of sodium dithionite in 20 mM Tris, 100 mM NaCl, pH 9.0. *C,* spectra of the C54S mutant were recorded in buffer C before (*solid line*) and after oxidation with an 1:1 molar ratio of ferricyanide (*dotted line*). The *g*-tensor determined by numerical simulation (data not shown) yields principal values as follows for *g*(1): 2.033, *g*(2): 2.018, *g*(3): 2.002 (error ± 0.002). All spectra were recorded at 40 μM protein concentration with the following parameters: microwave frequency, 9.424 GHz; microwave power, 8 milliwatt, field modulation frequency, 100 kHz, field modulation depth, 5 G (peak to peak); temperature 10 K.

Two [4Fe-4S]$^{2+}$ Clusters of ABCE1 Exist in Different Electronic Environments—To finally confirm the type of the two diamagnetic Fe-S clusters, WT ABCE1 was analyzed by Mössbauer spectroscopy. ABCE1 was labeled with ^{57}Fe in *S. solfataricus* and purified as described under the "Experimental Procedures." The Mössbauer spectrum of ABCE1 obtained at 77 K has been analyzed with three quadrupole doublets (Fig. 4*A*). Species 1 has an isomer shift of $\delta_1 = 0.43$ mm/s, a quadrupole splitting of $\Delta E_{Q1} = 1.32$ mm/s, and a relative contribution of 44%. Species 2 exhibits an isomer shift of $\delta_2 = 0.42$ mm/s, a quadrupole splitting of $\Delta E_{Q2} = -0.86$ mm/s, and also a relative contribution of 44%. The negative sign of ΔE_{Q2} has been determined by the analysis of the high field Mössbauer spectra (see Fig. 4*B*). The isomer shifts of species 1 and 2 are characteristic for $Fe^{2.5+}$ pairs of [4Fe-4S]$^{2+}$ clusters (25, 33).

Fig. 4*B* shows a Mössbauer spectrum of ABCE1 taken at 4.2 K in a field of 4 T perpendicular to the γ-beam. The observed magnetic splitting was successfully reproduced by the simula-

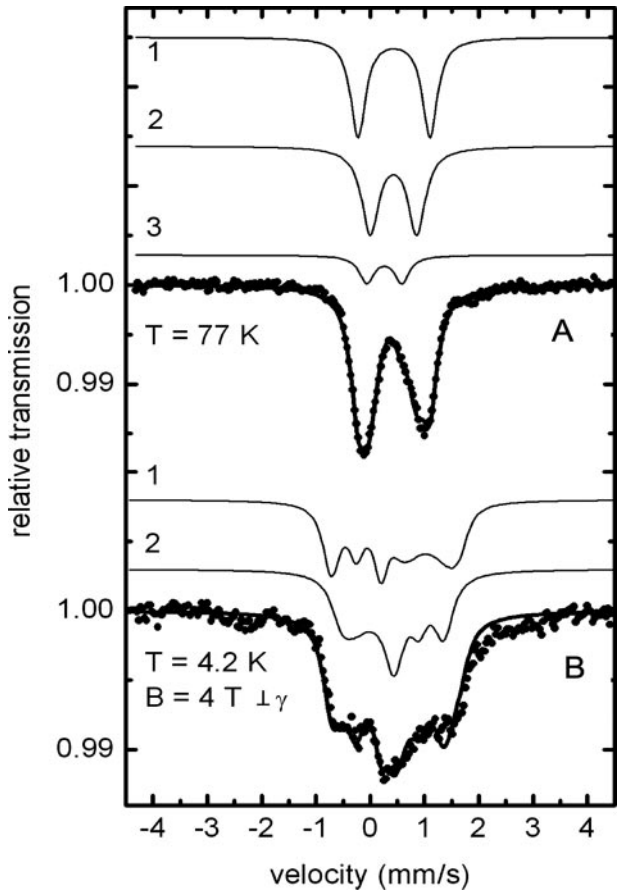

FIGURE 4. **Mössbauer spectroscopy of ABCE1.** Spectra of WT ABCE1 were recorded at 77 K in a zero magnetic field (*A*) and at 4.2 K in a field of 4 T perpendicular to the *g*-beam (*B*). The *solid lines* represent simulations with the parameters given under the "Experimental Procedures." Species 1 and 2, present at equimolar ratio (44% both), are diamagnetic and exhibit parameters typical for [4Fe-4S]$^{2+}$ clusters. Species 1, $\delta_1 = 0.43$ mm/s, $\Delta E_{Q1} = 1.32$ mm/s; species 2, $\delta_2 = 0.42$ mm/s, $\Delta E_{Q2} = -0.86$ mm/s. Species 3 (12%) is characteristic for unspecific Fe^{3+} and has been disregarded in the simulations shown in *B*. ABCE1 isolated from *S. solfataricus* was analyzed in buffer C at 1.2 mM in iron.

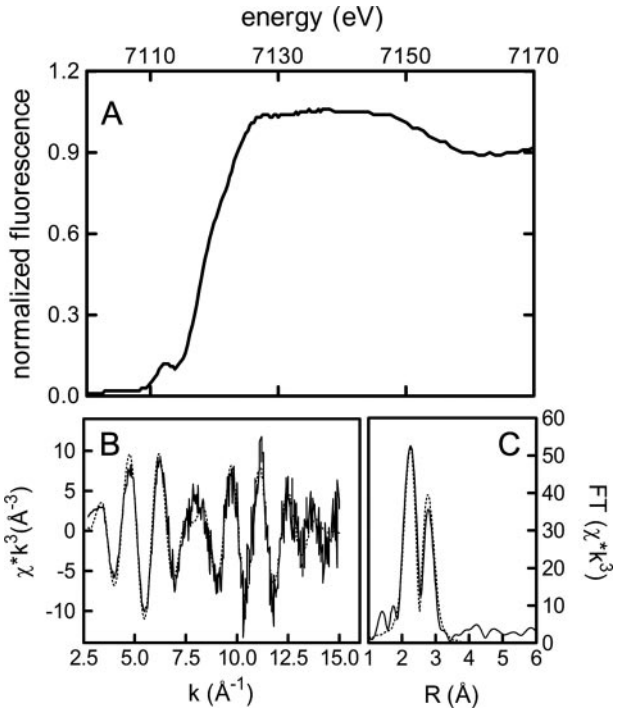

FIGURE 5. **X-ray absorption analysis of the Fe-S cluster in ABCE1.** *A,* iron *K*-edge x-ray absorption spectra of WT ABCE1 (*S. solfataricus*); *B,* iron *K*-edge k^3 weighed EXAFS spectra; and *C,* the corresponding Fourier transformation. The EXAFS is dominated by two contributions, the Fe-4S signal at 2.29 ± 0.01 Å and the Fe-3Fe signal at 2.74 ± 0.01 Å. The Debye-Waller factors (2 σ^2) for these contributions were refined to 0.010 ± 0.001 Å^2 and 0.008 ± 0.001 Å^2, respectively. Fermin energy (E_F) was −3 ± 1 eV. ABCE1 was analyzed in buffer C at an iron concentration of 1.2 mM.

tion shown in Fig. 4*B*. The input parameters for the simulation are the hyperfine parameters of components 1 and 2 as obtained from the analysis of the spectrum taken at 77 K (Fig. 4*A*) and show diamagnetic ground states of both species. This spectroscopic signature is again indicative for [4Fe-4S]$^{2+}$ clusters (25, 33). Species 3 with $\delta_3 = 0.26$ mm/s, $\Delta E_{Q3} = 0.63$ mm/s, and a relative contribution of 12% (Fig. 4*A*) does lead to a broad magnetic background in the high field spectrum. Such behavior is characteristic for an unspecific Fe^{3+} (33). Therefore, species 3 has been disregarded in the simulation. Considering the facts that iron quantification yields almost the amount of iron expected for two [4Fe-4S] clusters and that species 1 and 2 are present at an equal ratio, Mössbauer spectroscopy consistent with the model that ABCE1 has two [4Fe-4S]$^{2+}$ clusters in a slightly different electronic environment.

Coordination of Iron in the Clusters—The edge shape of the x-ray absorption near-edge structure spectra (Fig. 5*A*), which can be used as a fingerprint for the electronic structure of the metal ions, resembles the one reported for oxidized hydrogenase II from *Clostridium pasteurianum,* which harbors [4Fe-4S]$^{2+}$ clusters (34). Typical features are the resonance in the rising edge and the rather flat maximum followed by a sharp minimum. The extracted fine structure (EXAFS) is dominated by a single frequency with a shift at about 8 Å^{-1}. The high intensity at wave numbers larger than 10 Å^{-1} in biological samples indicates the presence of a multinuclear metal center. This is consistent with the peak at about 2.8 Å in the corresponding Fourier transformation (FT). The high intensity of the main peak at about 2.3 Å in the FT points toward a homogeneous first coordination sphere formed by sulfur ligands. The FT is very similar to the one observed for the [4Fe-4S]$^{2+}$ clusters mentioned above (34). Models based on the assumption of [4Fe-4S]$^{2+}$ clusters resemble the data very well (Fig. 5, *B* and *C*). All attempts to replace one of the sulfur ligands in the fit by light atoms such as oxygen or nitrogen lead to artificially long Fe-O/N distances. Thus, recognizable contributions above 10% of the average ligand sphere are excluded. The Fe-S distance of 2.29 Å and the Fe-Fe distances of 2.74 Å match the literature values for oxidized [4Fe-4S] clusters very well (35).

Essential Function of the Fe-S Clusters in ABCE1—By means of biophysical and biochemical analyses, we resolved that ABCE1 from *S. solfataricus* contains two diamagnetic [4Fe-4S]$^{2+}$ clusters. However, the functional impact of the two different Fe-S clusters cannot easily be addressed in Archaea. Therefore, we initiated a genetic analysis in *S. cerevisiae,* where ABCE1 has been shown to be essential for viability because of its fundamental role in translation initiation and ribosome biosynthesis (9, 12, 17). By systematic mutation of all conserved cysteine residues, individually or in combination, we addressed

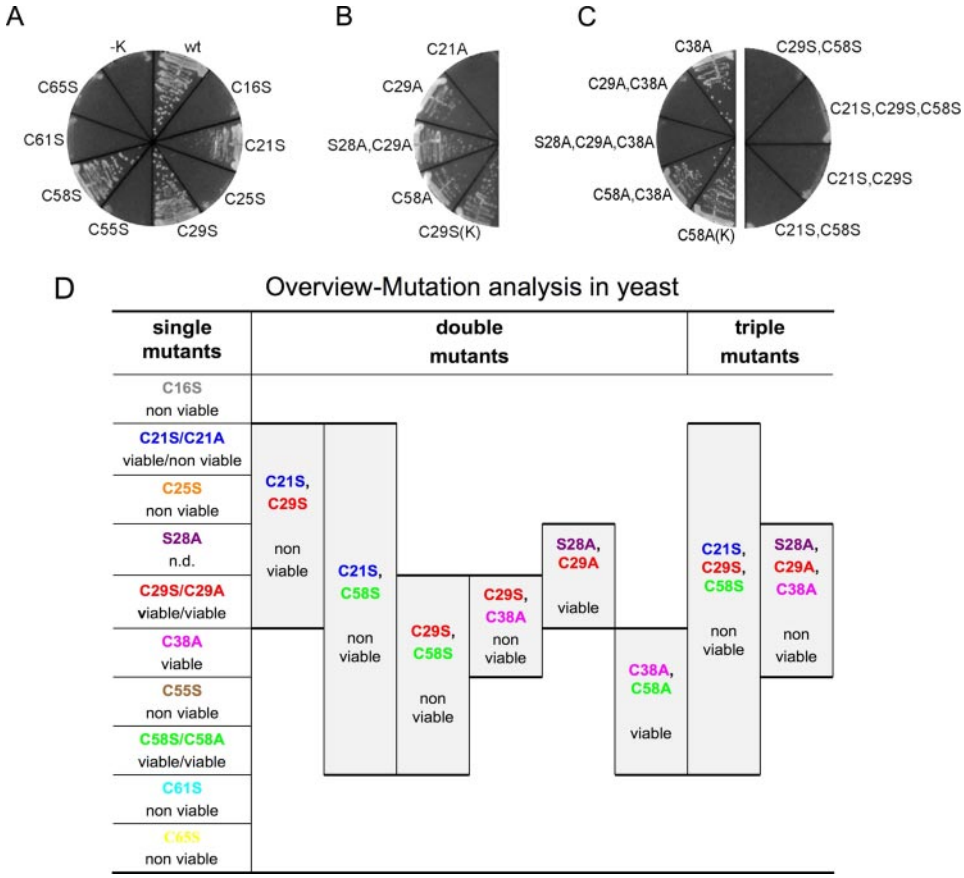

FIGURE 6. **Functional analysis of ABCE1 in *S. cerevisiae*.** Plasmids of ABCE1 harboring the indicated mutations were transformed into a yeast strain, in which the endogenous promoter was replaced by a tetracycline-repressible promoter and plated on minimal agar using histidine as a selection marker. Single colonies were then spread on minimal agar plates containing doxycycline. The plasmid containing WT ABCE1 served as a positive control (*wt*), and the empty vector as a negative control (−*K*). *A,* mutation of the eight conserved cysteine residues to serine. *B,* single cysteine-to-alanine mutations of the viable mutants from the first screen, as well as the double mutant S28A/C29A. *C,* mutation of the extra cysteine residue Cys-38 to alanine individually and in combination with selected conserved residues. Double and triple mutants of the viable mutants from the first screen are lethal. *D,* schematic overview of the cysteine mutation analysis in yeast.

the functional role of the Fe-S clusters in *S. cerevisiae* ABCE1. Plasmids encoding wild type or ABCE1 mutants were transformed into a yeast strain, in which a tetracycline-repressible one replaced the endogenous promoter of ABCE1. After repression of endogenous ABCE1 by addition of doxycycline, we analyzed single clones for viability.

Remarkably, only five of the eight conserved cysteines (Cys-16, Cys-25, Cys-55, Cys-61, and Cys-65; at positions 1, 3, 5, 7, and 8) were found to be essential for cell survival (Fig. 6*A*). To our surprise the C21S, C29S, and C58S mutants (at positions 2, 4, and 6) are still viable (Fig. 6*A*). It should be mentioned that the C21S mutant shows a slow growth phenotype. Because it is known that serine residues can coordinate Fe-S clusters in certain cases, we subsequently mutated each of these three cysteine residues to alanine. Here, C29A and C58A (at positions 4 and 6) were still viable, but the C21A mutant (at position 2) was lethal (Fig. 6*B*). In conclusion, six coordinating cysteines, of which serine at position 2 (C21S) can partially be accepted, are strictly required for the formation of the Fe-S clusters and cell survival. The inviability of the C25S and C61S mutant is in agreement with previous studies, which further demonstrated that substitution of these cysteines had no effect on the expression level and stability of the protein (9).

Interestingly, the viable yeast Cys-58 mutant corresponds to the C54S mutant in *S. solfataricus*. Biophysical and biochemical analyses indicate that this mutant contains a [4Fe-4S]$^{2+}$ and a paramagnetic [3Fe-4S]$^{+}$ center. In conclusion, the cysteine at position 6 is not essential for the assembly of the Fe-S cluster and vital function of ABCE1.

The viability of the Cys-29 mutants remained enigmatic, because the corresponding mutant in ABCE1 from *S. solfataricus* (C24S) showed a defect in Fe-S cluster assembly (see Figs. 1 and 2). We excluded that the adjacent Ser-28 rescues the Cys-29 mutation (Fig. 6*B*). However, by *in silico* analysis, we noticed that, in contrast to most archaeal homologues, all ABCE1 in Eukarya carry an extra cysteine in close proximity to the iron-sulfur centers. This corresponds to Cys-38 in *S. cerevisiae* ABCE1. In a process called ligand swapping, such a cysteine, originally not involved in Fe-S cluster coordination, can take over the function of a missing or mutated cysteine residue. To test this hypothesis, we generated the double C29A/C38A mutant. Indeed, this double mutation was lethal, whereas cells with the double mutation C58A/C38A as a control grew normally, demonstrating a site-specific ligand swapping between Cys-29 and Cys-38 (Fig. 6*B*).

Finally, double and triple mutants comprising the dispensable cysteines were generated. Notably, any combination of the otherwise viable mutations shows an additive effect, leading to a lethal phenotype (Fig. 6*C*).

DISCUSSION

The presence of Fe-S clusters discriminates the evolutionarily highly conserved protein ABCE1 from all other members of the ABC superfamily. In this study, we determined the type, coordination, and functional relevance of the Fe-S clusters in ABCE1 of Archaea and Eukarya. For detailed biophysical and biochemical analyses, we used ABCE1 from the hyperthermophilic crenarchaeote *S. solfataricus*, which contains only the eight conserved cysteine residues, putatively coordinating Fe-S clusters. By means of a novel expression system, ABCE1 was overexpressed and isolated from the homologous host, which ensured the complete machinery for Fe-S cluster assembly. Expression in *E. coli* was used to examine various mutants efficiently. The functional role of the Fe-S clusters was, however,

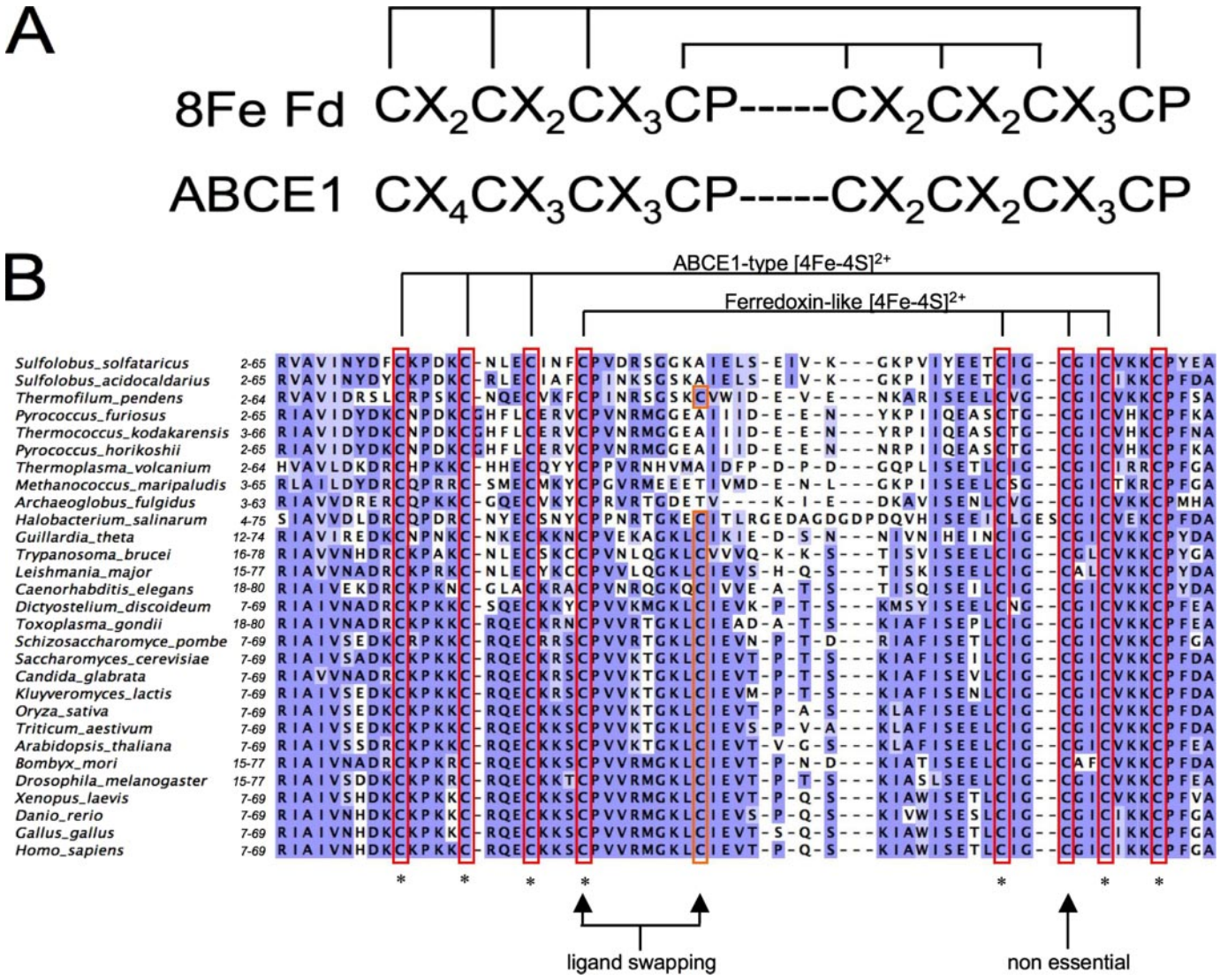

FIGURE 7. **Model for the structural organization of the Fe-S cluster in ABCE1.** *A,* consensus sequence of eight iron ferredoxins and the consensus sequence of Fe-S cluster in ABCE1 by comparison. *B,* sequence alignment of the N-terminal Fe-S cluster domain of ABCE1 from archaeal and eukaryotic organisms generated by ClustalW as follows: *S. solfataricus* (gi:15897231); *Sulfolobus acidocaldarius* (gi:70606479); *Thermofilum pendens* (gi:119719130); *Pyrococcus furiosus* (gi:18977042); *Thermococcus kodakarensis* (gi:57640966); *Pyrococcus horikoshii* (gi:14590719); *Thermoplasma volcanium* (gi:13542329); *Methanococcus maripaludis* (gi:45357945); *Archaeoglobus fulgidus* (gi:11497625); *Halobacterium salinarum* (gi:15791346); *Guillardia theta* (gi:13811968); *Trypanosoma brucei* (gi:21212953); *Leishmania major* (gi:68223887); *Caenorhabditis elegans* (gi:17555800); *Dictyostelium discoideum* (gi:66803577); *Toxoplasma gondii* (gi:111145381), *Schizosaccharomyces pombe* (gi:19113524); *S. cerevisiae* (gi:74676343); *Candida glabrata* (gi:50288565); *Kluyveromyces lactis* (gi:50306045); *Oryza sativa* (gi:115485837); *Tricitum aestivum* (gi:16755057); *Arabidopsis thaliana* (gi:110742163); *Bombyx mori* (gi:112982681); *Drosophila melanogaster* (gi:24661270); *Xenopus laevis* (gi:28302203); *Danio rerio* (gi:63102477); *Gallus gallus* (gi:57530144); and *Homo sapiens* (gi:987870). Essential cysteines are marked with an *asterisk*. Ligand swapping occurs between Cys-29 and the extra Cys-39, conserved among all eukaryotes. Cys-58 is not essential, because this cluster is also functional in a [3Fe-4S] state.

addressed in yeast, where ABCE1 is essential for cell viability (9, 12, 17).

The combination of structural and functional analyses clearly demonstrates the presence of two diamagnetic [4Fe-4S]$^{2+}$ clusters in ABCE1 and further highlights the essential role of the conserved cysteines for Fe-S cluster assembly. Sequence comparison shows that the Fe-S cluster coordination in ABCE1 (Fig. 7*A*) partially resembles those of eight iron ferredoxins, *e.g.* in *Desulfovibrio africanus* ferredoxin III or *Azotobacter vinelandii* ferredoxin I (36, 37). We therefore conclude that ABCE1 contains one ferredoxin-like [4Fe-4S]$^{2+}$ cluster formed by the cysteines at positions 4–7. Indeed, this cluster perfectly matches the ferredoxin-type consensus sequence $CPX_nCX_2CX_2C$ (Fig. 7*B*). The coordination of the second Fe-S cluster in ABCE1 (cysteines at positions 1–3 and 8) has not been described in any other protein. Hence, we propose a unique ABCE1-type [4Fe-4S]$^{2+}$ cluster with the consensus sequence $CXPX_2CX_3CX_nKCP$. This model shall be clarified by a high resolution structure of the full-length protein.

Both clusters are equally present but have a slightly different electronic environment as demonstrated by Mössbauer spectroscopy (see Fig. 4). Based on the quadrupole splitting, species 1 ($\delta_1 = 0.43$ mm/s, $\Delta E_{Q1} = 1.32$ mm/s) is typical for a ferredoxin-like cluster (38, 39), whereas species 2 ($\delta_2 = 0.42$ mm/s, $\Delta E_{Q2} = -0.86$ mm/s) should reflect the ABCE1-type cluster. Additional atoms, such as oxygen or nitrogen from aspartate, histi-

TABLE 1
Iron and sulfur determination from ABCE1 (1 nmol)

	Iron		Inorganic sulfur, methylene blue	Total sulfur, TXRF
	Ferrozine	TXRF		
	nmol		*nmol*	*nmol*
WT (*S. solfataricus*)	7.2 ± 0.5	6.8 ± 0.3	6.1 ± 0.2	25.0 ± 0.6
WT (*E. coli*)	6.2 ± 0.2	6.0 ± 0.2	5.5 ± 0.1	21.8 ± 0.6
C54S (*E. coli*)	4.4 ± 0.1	ND[a]	3.1 ± 0.1	ND
C24S (*E. coli*)	ND	0.4 ± 0.1	0.0 ± 0.0	12.1 ± 0.6

[a] ND indicates not done.

dine, or serine residues, for example, do not contribute to the cluster coordination in WT ABCE1 and the C54S mutant, according to both XAS and ESEEM analysis.

The systematic mutagenesis of all conserved cysteines in ABCE1 revealed that, surprisingly, three cysteine-to-serine mutants (C21S, C29S, and C58S) are not lethal. The C21S mutant has a slow growth phenotype, demonstrating that serine at position 2 can partially substitute cysteine in coordination and assembly of the Fe-S clusters. Nevertheless, four sites (position 1–3 and 8) are strictly required for formation of the ABCE1-type cluster and ABCE1 function (see Fig. 6).

In contrast, position 6, which is part of the ferredoxin-like cluster, is dispensable for the essential ABCE1 function. Strikingly, this cluster can also exist in a [3Fe-4S]$^{+}$ state. Although interconversion between [4Fe-4S] and [3Fe-4S] clusters has been reported, as, for example, in the ferredoxin II form *Desulfovibrio gigas* (39) or ferredoxin III from *D. africanus* (36), we have at present no evidence of whether this state exists for WT ABCE1 *in vivo*. Remarkably, the mutant at position 6 was extremely labile toward oxidation, resulting in a loss of iron and acid-labile sulfur. These findings further support the "all-or-nothing" behavior of the two Fe-S clusters in ABCE1, meaning that they assemble simultaneously and depend on each other (9). Double and triple mutants of the dispensable positions display additive effects resulting in lethality (see Fig. 6). The fact that the Fe-S clusters in ABCE1 are stable down to redox potentials of approximately $E'_0 = -560$ mV and that the ferredoxin-like cluster is functional in different states indicates a structural rather than redox-catalytic role for this cluster, similar to *E. coli* endonucleases III (40). In this enzyme, the Fe-S cluster serves as a scaffold for proper positioning of catalytic amino acids involved in DNA recognition and binding. Notably, the N-terminal Fe-S domains of ABCE1 are rich in conserved basic residues, which could, similarly to the *E. coli* endonuclease III or MutY, sense and modify nucleic acids (40–42). Despite the potential role in scaffolding a ligand-binding site, the Fe-S clusters of ABCE1 are not required for the folding and the structural integrity of the twin ABC ATPase domains (14). From the x-ray structure it was anticipated that the two nucleotide binding domains perform an ATP-driven clamp-like motion. Nevertheless, the impact of the Fe-S domain on conformation changes and the ATP hydrolysis cycle of ABCE1 needs to be addressed in future experiments.

The dispensable cysteine at position 4 of yeast ABCE1(C29A or C29S) is remarkable, because the corresponding mutation in *S. solfataricus* ABCE1 (C24S) completely abolishes the incorporation of iron and acid-labile sulfur (see Table 1 and Figs. 1 and 2). Strikingly, all eukaryotic ABCE1 proteins contain a conserved extra cysteine within the N-terminal Fe-S cluster domain, which can rescue Cys-29 (position 4) by ligand swapping. This extra cysteine, absent in most Archaea, explains why the mutation at position 4 (C24S) in *S. solfataricus* ABCE1 showed no assembled Fe-S clusters. Noteworthy, mutation of Cys-38 (extra cysteine) has no effect on ABCE1 function in yeast. It is therefore questionable if ligand swapping occurs *in vivo*.

ABC-type proteins are evolutionarily highly conserved molecular machines, coupling ATP binding and hydrolysis to conformational changes (43, 44). The smallest functional unit appears to be an ABC dimer, which operates in a processive engagement/disengagement cycle (44–46). These chemomechanical engines drive not only membrane translocation but also a variety of other crucial biological processes, such as DNA repair and chromosome segregation. The fundamental role of ABCE1 in RNase L inhibition, human immunodeficiency virus capsid maturation, translation initiation, and ribosome biosynthesis (8, 12, 13, 15–17) suggests that the two essential diamagnetic [4Fe-4S]$^{2+}$ clusters identified in this study are involved in recognition and modification (chemical or conformational) of RNA assemblies.

Acknowledgments—We thank Volker Müller and Beate Averhoff (Institute of Molecular Biosciences, Goethe University, Frankfurt) for the opportunity to use the S. solfataricus fermentation facility and the anaerobic chamber and Eckhard Boles (Institute of Molecular Biosciences, Goethe University, Frankfurt) for many helpful comments. We are also grateful to Bernd O. Kolbesen and Claudia Rittmeyer (Institute of Inorganic and Analytical Chemistry, Goethe University, Frankfurt) for TXRF measurements. We thank Thomas Prisner (Institute of Physical and Theoretical Chemistry, Goethe University, Frankfurt) for access to the EPR instrumentation. We further acknowledge Chiara Presenti for excellent assistance. Financial support by the Center for Membrane Proteomics at the Goethe University, Frankfurt, is kindly acknowledged.

REFERENCES

1. Beinert, H., Holm, R. H., and Munck, E. (1997) *Science* **277,** 653–659
2. Howard, J. B., and Rees, D. C. (2006) *Proc. Natl. Acad. Sci. U. S. A.* **103,** 17088–17093
3. Khoroshilova, N., Popescu, C., Munck, E., Beinert, H., and Kiley, P. J. (1997) *Proc. Natl. Acad. Sci. U. S. A.* **94,** 6087–6092
4. Pierrel, F., Douki, T., Fontecave, M., and Atta, M. (2004) *J. Biol. Chem.* **279,** 47555–47563
5. Zheng, L., and Dean, D. R. (1994) *J. Biol. Chem.* **269,** 18723–18726
6. Lill, R., and Muhlenhoff, U. (2006) *Annu. Rev. Cell Dev. Biol.* **22,** 457–486
7. Lill, R., Fekete, Z., Sipos, K., and Rotte, C. (2005) *IUBMB Life* **57,** 701–703
8. Kispal, G., Csere, P., Prohl, C., and Lill, R. (1999) *EMBO J.* **18,** 3981–3989
9. Kispal, G., Sipos, K., Lange, H., Fekete, Z., Bedekovics, T., Janaky, T., Bassler, J., Aguilar Netz, D. J., Balk, J., Rotte, C., and Lill, R. (2005) *EMBO J.* **24,** 589–598
10. Braz, A. S., Finnegan, J., Waterhouse, P., and Margis, R. (2004) *J. Mol. Evol.* **59,** 20–30
11. Zhao, Z., Fang, L. L., Johnsen, R., and Baillie, D. L. (2004) *Biochem. Biophys. Res. Commun.* **323,** 104–111
12. Yarunin, A., Panse, V. G., Petfalski, E., Dez, C., Tollervey, D., and Hurt, E. C. (2005) *EMBO J.* **24,** 580–588
13. Chen, Z. Q., Dong, J., Ishimura, A., Daar, I., Hinnebusch, A. G., and Dean, M. (2006) *J. Biol. Chem.* **281,** 7452–7457
14. Karcher, A., Buttner, K., Martens, B., Jansen, R. P., and Hopfner, K. P.

(2005) *Structure* (*Camb.*) **13,** 649–659
15. Bisbal, C., Martinand, C., Silhol, M., Lebleu, B., and Salehzada, T. (1995) *J. Biol. Chem.* **270,** 13308–13317
16. Zimmerman, C., Klein, K. C., Kiser, P. K., Singh, A. R., Firestein, B. L., Riba, S. C., and Lingappa, J. R. (2002) *Nature* **415,** 88–92
17. Dong, J., Lai, R., Nielsen, K., Fekete, C. A., Qiu, H., and Hinnebusch, A. G. (2004) *J. Biol. Chem.* **279,** 42157–42168
18. Albers, S. V., Jonuscheit, M., Dinkelaker, S., Urich, T., Kletzin, A., Tampé, R., Driessen, A. J., and Schleper, C. (2006) *Appl. Environ. Microbiol.* **72,** 102–111
19. Jonuscheit, M., Martusewitsch, E., Stedman, K. M., and Schleper, C. (2003) *Mol. Microbiol.* **48,** 1241–1252
20. Schleper, C., Kubo, K., and Zillig, W. (1992) *Proc. Natl. Acad. Sci. U. S. A.* **89,** 7645–7649
21. Martusewitsch, E., Sensen, C. W., and Schleper, C. (2000) *J. Bacteriol.* **182,** 2574–2581
22. Albers, S. V., Szabo, Z., and Driessen, A. J. (2003) *J. Bacteriol.* **185,** 3918–3925
23. Fish, W. W. (1988) *Methods Enzymol.* **158,** 357–364
24. Beinert, H. (1983) *Anal. Biochem.* **131,** 373–378
25. Schünemann, V., and Winkler, H. (2000) *Rep. Prog. Phys.* **63,** 263–353
26. Korbas, M., Marsa, D. F., and Meyer-Klaucke, W. (2006) *Rev. Sci. Instrum.* **77,** 063105-1–063105-5
27. Korbas, M., Vogt, S., Meyer-Klaucke, W., Bill, E., Lyon, E. J., Thauer, R. K., and Shima, S. (2006) *J. Biol. Chem.* **281,** 30804–30813
28. Hughes, J. D., Estep, P. W., Tavazoie, S., and Church, G. M. (2000) *J. Mol. Biol.* **296,** 1205–1214
29. Khoroshilova, N., Beinert, H., and Kiley, P. J. (1995) *Proc. Natl. Acad. Sci. U. S. A.* **92,** 2499–2503
30. Orme-Johnson, W. H., and Orme-Johnson, N. R. (1982) in *Iron-Sulfur Proteins* (Spiro, R. G., ed) pp. 67–96, Wiley Interscience, New York
31. Elsasser, C., Brecht, M., and Bittl, R. (2002) *J. Am. Chem. Soc.* **124,** 12606–12611
32. Agarwalla, S., Stroud, R. M., and Gaffney, B. J. (2004) *J. Biol. Chem.* **279,** 34123–34129
33. Seemann, M., Wegner, P., Schunemann, V., Bui, B. T., Wolff, M., Marquet, A., Trautwein, A. X., and Rohmer, M. (2005) *J. Biol. Inorg. Chem.* **10,** 131–137
34. George, G. N., Prince, R. C., Stokley, K. E., and Adams, M. W. (1989) *Biochem. J.* **259,** 597–600
35. Stout, C. D. (2001) in *Handbook of Metalloproteins* (Messerschmidt, A., Huber, R., Wieghardt, K., and Poulos, T., eds) pp. 560–573, Wiley Interscience, New York
36. Busch, J. L., Breton, J. L., Bartlett, B. M., Armstrong, F. A., James, R., and Thomson, A. J. (1997) *Biochem. J.* **323,** 95–102
37. Tilley, G. J., Camba, R., Burgess, B. K., and Armstrong, F. A. (2001) *Biochem. J.* **360,** 717–726
38. Emptage, M. H., Kent, T. A., Huynh, B. H., Rawlings, J., Orme-Johnson, W. H., and Munck, E. (1980) *J. Biol. Chem.* **255,** 1793–1796
39. Moura, J. J., Moura, I., Kent, T. A., Lipscomb, J. D., Huynh, B. H., LeGall, J., Xavier, A. V., and Munck, E. (1982) *J. Biol. Chem.* **257,** 6259–6267
40. Kuo, C. F., McRee, D. E., Fisher, C. L., O'Handley, S. F., Cunningham, R. P., and Tainer, J. A. (1992) *Science* **258,** 434–440
41. Porello, S. L., Cannon, M. J., and David, S. S. (1998) *Biochemistry* **37,** 6465–6475
42. Thayer, M. M., Ahern, H., Xing, D., Cunningham, R. P., and Tainer, J. A. (1995) *EMBO J.* **14,** 4108–4120
43. Hopfner, K. P., and Tainer, J. A. (2003) *Curr. Opin. Struct. Biol.* **13,** 249–255
44. Schmitt, L., and Tampé, R. (2002) *Curr. Opin. Struct. Biol.* **12,** 754–760
45. Janas, E., Hofacker, M., Chen, M., Gompf, S., van der Does, C., and Tampé, R. (2003) *J. Biol. Chem.* **278,** 26862–26869
46. van der Does, C., and Tampé, R. (2004) *Biol. Chem.* **385,** 927–933